Cell Metabolism
Short Article

Deficiency of Lipoprotein Lipase in Neurons Modifies the Regulation of Energy Balance and Leads to Obesity

Hong Wang,[1] Giuseppe Astarita,[2] Matthew D. Taussig,[1] Kalyani G. Bharadwaj,[5] Nicholas V. DiPatrizio,[2] Klaus-Armin Nave,[3] Daniele Piomelli,[2,4] Ira J. Goldberg,[5] and Robert H. Eckel[1,*]
[1]Division of Endocrinology, Metabolism, and Diabetes, Department of Medicine, University of Colorado, Denver Anschutz Medical Campus, Aurora, CO 80045, USA
[2]Department of Pharmacology, University of California, Irvine, Irvine, CA 92617, USA
[3]Department of Neurogenetics, Max-Planck-Institute of Experimental Medicine, 37075 Goettingen, Germany
[4]Drug Discovery and Development, Italian Institute of Technology, 16163 Genoa, Italy
[5]Department of Medicine, Columbia University, New York, NY 10032, USA
*Correspondence: robert.eckel@ucdenver.edu
DOI 10.1016/j.cmet.2010.12.006

SUMMARY

Free fatty acids (FFAs) suppress appetite when injected into the hypothalamus. To examine whether lipoprotein lipase (LPL), a serine hydrolase that releases FFAs from circulating triglyceride (TG)-rich lipoproteins, might contribute to FFA-mediated signaling in the brain, we created neuron-specific LPL-deficient mice. Homozygous mutant (NEXLPL−/−) mice were hyperphagic and became obese by 16 weeks of age. These traits were accompanied by elevations in the hypothalamic orexigenic neuropeptides, AgRP and NPY, and were followed by reductions in metabolic rate. The uptake of TG-rich lipoprotein fatty acids was reduced in the hypothalamus of 3-month-old NEXLPL−/− mice. Moreover, deficiencies in essential fatty acids in the hypothalamus were evident by 3 months, with major deficiencies of long-chain n-3 fatty acids by 12 months. These results indicate that TG-rich lipoproteins are sensed in the brain by an LPL-dependent mechanism and provide lipid signals for the central regulation of body weight and energy balance.

INTRODUCTION

Substantial evidence indicates the essential role of the central nervous system (CNS) in the regulation of energy homeostasis, leading to obesity development (Schwartz and Porte, 2005). Among the various brain regions involved, the hypothalamus plays a critical role in integrating neuronal responses to a variety of peripheral signals to regulate energy balance. In the arcuate nucleus of the hypothalamus, two groups of neurons, pro-opiomelanocortin (POMC)-producing neurons and agouti-related protein (AgRP)-producing neurons, play complementary roles in regulating food intake, energy expenditure, and body weight (Sandoval et al., 2008). While the glucose-sensing mechanism in POMC neurons and its role in obesity is well defined (Parton et al., 2007), the mechanism and the locations for lipid/fatty acid (FA) sensing in the brain are less clear, and how the imbalance of central versus peripheral lipid-sensing contributes to the development of obesity is poorly understood (Caspi et al., 2007).

FA availability in the hypothalamus is important to the regulation of energy balance, but how the brain regulates the de novo synthesis versus the transport of FAs into the brain is unclear. In recent years, studies with the infusion of free fatty acids (FFAs) into the third ventricle of rodents showed inhibition of food intake (Obici et al., 2002; Morgan et al., 2004) as well as regulation of enzymes that are essential to FA oxidation (Obici et al., 2003) and lipogenesis (Loftus et al., 2000) that affect energy balance mostly through appetite regulation. The in vivo sources of these appetite-regulating FAs and the regulatory mechanisms remain undefined. Furthermore, appetite suppression by FFAs seems to be contrary to known physiologic appetite regulation such as starvation (circulating FFAs are increased) and fed state (FFAs are suppressed). Thus, brain lipids, specifically hypothalamic FAs, might be regulated differently and independently of the circulating FFAs. The major pools of circulating FAs are either albumin-bound FFAs released by lipolysis from adipose tissue TG storage pools or FFAs contained within TG-rich lipoproteins that increase in the blood after meals. A physiologically relevant model is critically necessary to study whether TG-rich lipoproteins could be a major source of FAs in the brain and whether the regulation of TG-rich lipoprotein metabolism in the brain affects energy balance.

Lipoprotein lipase (LPL) is a key enzyme that controls the partitioning of TG-rich, lipoprotein-derived FAs in peripheral tissues (Wang and Eckel, 2009). LPL mRNA is also present throughout the nervous system, including CNS neurons (Goldberg et al., 1989; Ben Zeev et al., 1990; Bessesen et al., 1993). A number of functions of LPL in neurons have been suggested (reviewed in Wang and Eckel, 2009); however, a relevant model is lacking to study the in vivo function of LPL in the brain. The neuron-specific, LPL-deficient mouse (NEXLPL−/−) reported here provides evidence that the regulation of TG-rich lipoprotein metabolism in the brain impacts both food intake and energy expenditure and results in obesity.

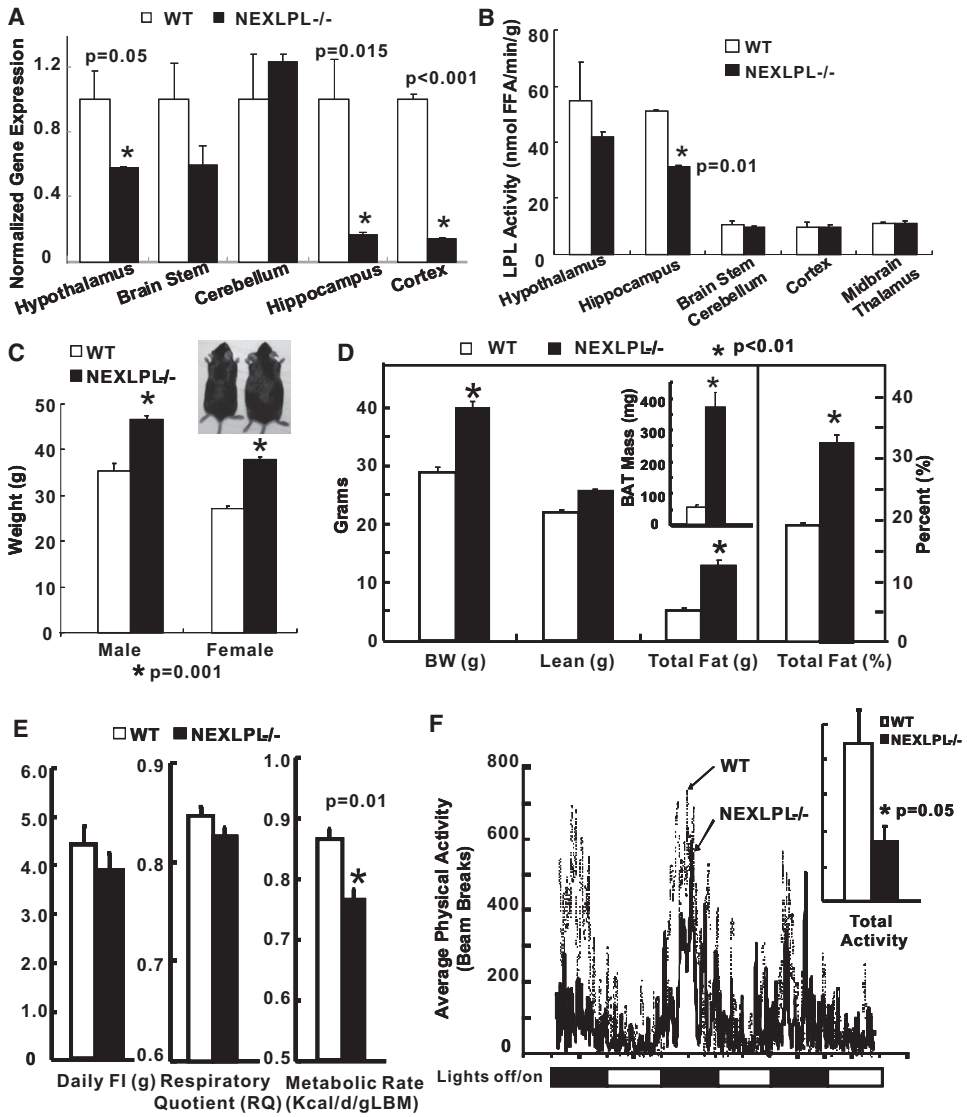

Figure 1. Characterization of NEXLPL–/– Mice

(A) Lipoprotein lipase (LPL) mRNA in different brain regions at 3 months (n = 4).

(B) LPL activity in different brain regions at 3 months (n = 3).

(C) Body weight for male and female NEXLPL mice at 6 months.

(D) Body composition and fat mass for NEXLPL mice at 6 months (insert: BAT mass).

(E) Energy balance of NEXLPL−/− mice at 6 months. Average daily food intake, respiratory quotient, and metabolic rate were measured in an indirect calorimeter.

(F) Average physical activity as measured by the number of breaks in inferred beams through the 3 day calorimetry experiment (insert: average total physical activity). n = 6 for (C)–(F). See also Figure S1 and Table S1. The error bars in this figure are SEM.

RESULTS

NEXLPL–/– Mice Become Obese on a Chow Diet

In 3-month-old NEXLPL−/− mice, LPL mRNA was significantly reduced in the hypothalamus (50%, p = 0.05), hippocampus (80%, p = 0.015), and cortex (80%, p < 0.001) (Figure 1A). However, LPL enzyme activity was reduced only 50% in the hippocampus and marginally in the hypothalamus and remained the same for other brain regions examined (Figure 1B). In peripheral tissues, the only change observed was an increase of LPL mRNA in BAT at 3 months (mechanism unknown, but unlikely a direct effect of genetic modification), with no enzyme activity changes in the heart, skeletal muscle, WAT, or BAT (Figures S1A and S1B).

At 6 months, obesity was observed in chow-fed male and female NEXLPL−/− mice, and female mice showed higher percent weight gain than male mice (Figure 1C) (38% versus 29%). Although some increase in lean body mass was seen (consistent with human obesity), most of the weight increase was fat mass (Figure 1D). Visual inspection of NEXLPL−/− mice revealed increases in the abdominal and perigonadal WAT areas and suprascapular BAT (quantified in Figure 1D

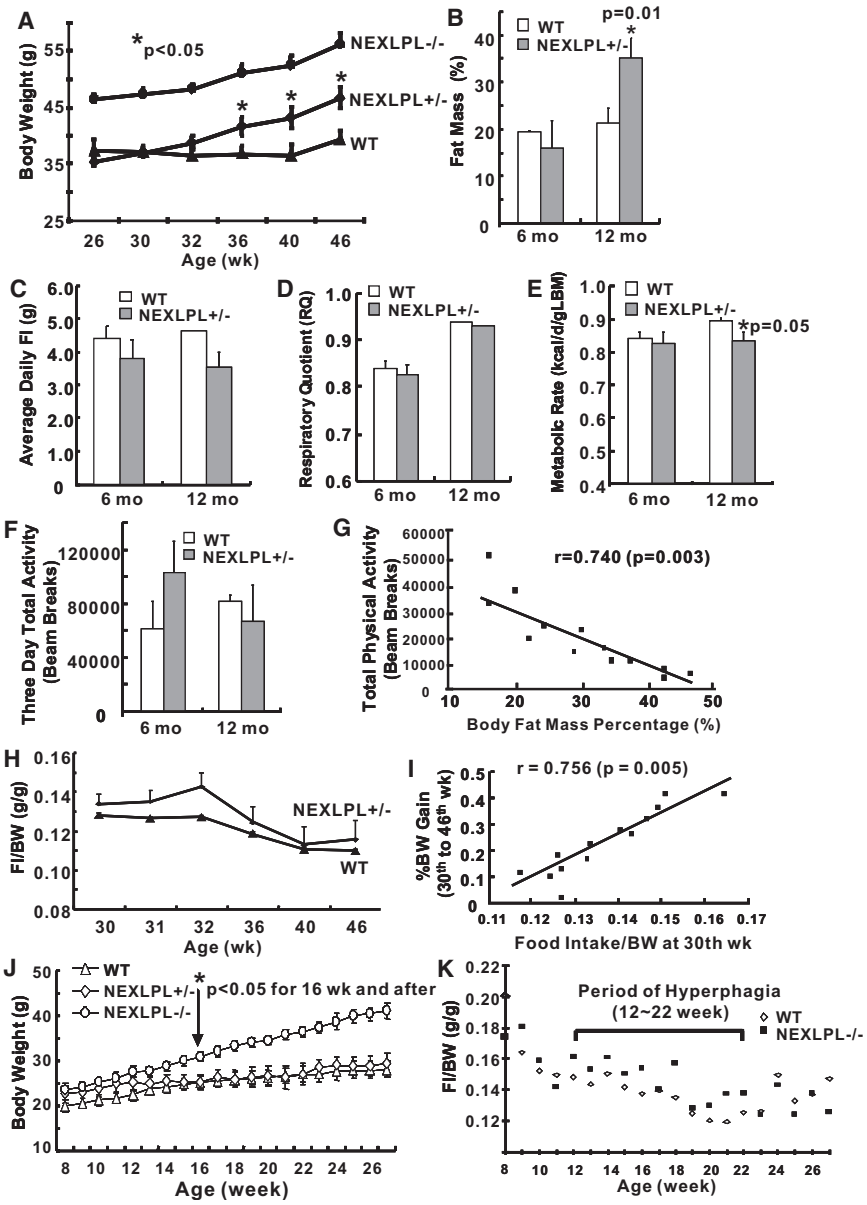

Figure 2. Obesity Development in NEXLPL+/– and NEXLPL–/– Mice

(A) Weight changes of NEXLPL+/– and NEXLPL–/– mice from 6 to 12 months (n = 4 for WT, n = 9 for NEXLPL+/–, n = 4 for NEXLPL–/–).

(B) Fat mass percentages of NEXLPL+/– mice at 6 and 12 months (n = 4 for 6 months, n = 4 for WT, n = 9 for NEXLPL+/– at 12 months).

(C) Average food intake for NEXLPL+/– mice at 6 and 12 months (n = 8 for WT, n = 13 for NEXLPL+/– at 6 months, n = 4 for WT, n = 9 for NEXLPL+/– at 12 months).

(D) Average respiratory quotient (RQ) for NEXLPL+/– mice at 6 and 12 months (same n numbers as in C.)

(E) Average metabolic rate (MR) for NEXLPL+/– mice at 6 and 12 months (same n numbers as in C).

(F) Total 3 day activity during the calorimetry experiment for NEXLPL+/– mice at 6 months and 12 months (same n number as in C).

(G) Correlation between total physical activities versus body fat mass percentage for NEXLPL+/– mice at 12 months (n = 4 for WT, n = 9 for NEXLPL+/–).

(H) Food intake increase before obesity in NEXLPL+/– mice (n = 4 for WT, n = 9 for NEXLPL+/–, n = 4 for NEXLPL–/–).

(I) Correlation between the weight gain at 46 weeks versus food intake at 30 weeks for NEXLPL+/– mice (n = 4 for WT, n = 9 for NEXLPL+/–).

(J) Weight changes of NEXLPL–/– and NEXLPL+/– mice between 8 weeks and 6 months of age (n = 8 for WT, n = 4 for NEXLPL+/–, n = 8 for NEXLPL–/–).

(K) Food intake increase before obesity in NEXLPL–/– mice (same n numbers as in J). The error bars in this figure are SEM.

insert). Other organs/tissues appeared to be anatomically normal. Indirect calorimetric characterization of energy balance showed no difference in average daily food intake (Figure 1E) and average respiratory quotient (RQ) between NEXLPL–/– and WT mice (Figure 1E). However, the average metabolic rate (MR) was lower in 6-month-old NEXLPL–/– mice (Figure 1E). Furthermore, NEXLPL–/– mice displayed a substantial reduction in physical activity (Figure 1F and insert). NEXLPL–/– mice at 6 months also showed varied but consistent reductions in LPL mRNA and enzyme activities in brain regions versus 3 months (Figures S1C and S1D). LPL mRNA levels seemed to be reduced in both WAT and BAT at 6 months (Figure S1E), but LPL activities in peripheral tissues were similar to those in 3-month-old NEXLPL–/– mice (Figure S1F).

Energy Intake and Energy Expenditure Are Both Modified in NEXLPL+/– and Young NEXLPL–/– Mice

Heterozygous mice (NEXLPL+/–) initially showed no differences in weight compared to WT mice at 6 months, but variably developed obesity as they aged (Figure 2A). The extra weight gain of 12-month-old NEXLPL+/– mice was also fat mass, similar to NEXLPL–/– mice at 6 months (Figure 2B). Indirect calorimetry showed no differences in food intake (Figure 2C) and RQ at either 6 or 12 months (Figure 2D). The MRs remained the same at 6 months and were modestly reduced at 12 months (Figure 2E). There was a large variance in physical activity for both 6- and 12-month-old NEXLPL+/– mice (Figure 2F), and the variance in the reductions of physical activity at 12 months reflected the degree of obesity (Figure 2G).

A short period of increased food intake was observed between the 30th and 32nd weeks (Figure 2H) for NEXLPL+/– mice. Food intake returned to the level of WT mice at 36 weeks, when the NEXLPL+/– started to become obese and remained low as the mice aged and further accumulated fat mass. Of great interest, the later development of obesity in NEXLPL+/– mice was

strongly predicted by the earlier increase in food intake at week 30 (Figure 2I). Thus, the development of obesity in NEXLPL+/− mice followed a two-step time course: a period of hyperphagia followed by a reduction in MR and physical activity. Obesity developed at a much faster pace in NEXLPL−/− mice (Figure 2J), with additional weight gain observed at 16 weeks. The pattern of earlier food intake for NEXLPL−/− mice was not as distinctive as that for NEXLPL+/−, but clearly began before the obesity developed, as well (Figure 2K).

Plasma metabolites were measured for 3- and 6-month-old male and female NEXLPL−/− mice. Insulin and leptin levels were higher in 6-month-old females, but fasting plasma glucose, FFA, and TG were normal both pre- (3 months) and post- (6 months) obesity (Table S1). At 3 months, fasting plasma insulin was minimally increased in both female and male NEXLPL−/− versus WT mice, but at 6 months, the fasting insulin and leptin levels were much less elevated in male than female NEXLPL−/− mice, despite both male and female NEXLPL−/− mice developing obesity on similar time courses. For all other comparisons, there were no clear sex differences observed.

Defect in Uptake and Metabolism of TG-Rich Lipoproteins in the Hypothalamus of NEXLPL–/– Mice

To address how neuronal LPL-deficient mice process circulating TG-rich lipoprotein-derived FAs, radiolabeled triolein tracer was incorporated endogenously into chylomicrons (CMs), and the labeled CMs were then injected into NEXLPL−/− and WT mice. Tissue uptake of the TG tracer was measured in various brain regions as well as peripheral tissues (Figure S2A). In peripheral tissues, BAT and liver had higher amounts of uptake of TG tracer than heart and WAT. Noteworthy specific brain regions such as the hypothalamus and hippocampus had amounts of TG tracer uptake similar to WAT. This clearly indicated that TG-rich lipoprotein-derived FAs enter the brain, and most importantly, this uptake was significantly reduced in the hypothalamus of NEXLPL−/− but not in other brain regions (Figure 3A).

Lipidomic analysis was conducted in the hypothalamus of 3- and 6-month-old NEXLPL−/− and WT mice to assess the impact of neuronal LPL deficiency on brain lipid metabolism. Total plasma concentrations of TG and FFA (Table S2) as well as individual species were similar at 3 and 6 months. These data resembled those measured in plasma (Table S1). When normalizing to plasma values, total TG (Figure 3B) was reduced in the hypothalamus of 3-month-old NEXLPL−/− mice and remained low at 6 months. One linoleic acid (18:2)-containing TG molecule (14:0/18:2/16:0) was dramatically reduced in the hypothalamus of 3-month-old NEXLPL−/− mice (Figure 3C) but was not changed in plasma (Table S2). Although total FFA levels were similar in NEXLPL−/− and WT mice at both 3 and 6 months (Figure 3D), reductions in n-3 polyunsaturated fatty acids (PUFAs) were detected (Figure 3E). In addition, an increase in C20:3 n-9 FFA, an additional marker of essential FA deficiency (Smit et al., 2004), was also seen at 3 months (Figure 3E). The detailed TG and FFA analysis in the hypothalamus is shown in Table S2. These data suggest that young NEXLPL−/− mice might have a specific deficiency in the brain uptake of TG-derived lipids.

This earlier defect seemed to manifest in 12-month-old NEXLPL−/− mice. There was a trend for the levels of hypothalamic total TG and specific TG molecules to be higher (Figures S2B and S2C); however, total FFA concentrations remained unchanged, as did the more abundant FFA species (Figure S2D). Also consistent with data from younger mice, the levels of very-long-chain PUFAs were all substantially lower in NEXLPL−/− mice, with dramatic reductions in n-3 PUFAs (Figure 3F). In addition, the C20:4 n-6-containing TGs were trending higher in NEXLPL−/− mice (Figure S2E), whereas the C20:4 n-6-containing diacylglycerol (DG) (Figure S2F), monoacylglycerol (MG) (Figure S2G), and C20:4 FFA (Figure S2H) species were all lower or trending lower. Taken together, these results suggest that NEXLPL−/− mice have a hypothalamic defect in metabolizing TG into DG, MG, and FFA, and more importantly, this impairment seems to be specific for very-long-chain PUFAs.

Key enzymes in the PUFA synthetic pathway were examined next in both the hypothalamus (Figure 3G) and liver (Figure S2I). Of interest, none of the desaturases or elongases were different in the hypothalamus at 3 months, but significant increases were observed for Fads1 (Δ-5 desaturase), Elovl 2 (elongase 2), and stearoyl-CoA desaturase 1 (Scd1) in the hypothalamus of 6-month-old NEXLPL−/− mice, and the elevation in Fads1 expression persisted in NEXLPL−/− mice at 12 months (Figure S2J). Liver PUFA biosynthetic enzymes were not modified except for the increase of Elovl2 at 3 months (Figure S2I).

Alterations of Gene Expression in the Hypothalamus of NEXLPL–/– and NEXLPL+/– Mice

To determine mechanisms by which neuronal LPL deficiency might modify energy balance and body weight, mRNA levels of a selected group of genes involved in CNS glucose sensing, lipid metabolism, energy balance, and body weight regulation were variably examined in the hypothalamus at 3 and 6 months (Figures S3A and S3B), and in the hippocampus (Figure S3C) and cortex (Figure S3D) at 6 months. With the exception of the mRNAs for sterol regulatory element-binding protein-1c (Srebp-1c), Srebp-2, carnitine palmitoyltransferase 1c (Cpt1c), and pyruvate dehydrogenase kinase (Pdk4) in the hypothalamus and Cpt1c, AMP-activated protein kinase alpha 2, and uncoupling protein 2 in cortex, no other changes were seen in 6-month-old NEXLPL−/− mice. At 3 months, some increases in medium-chain acyl-CoA dehydrogenase and Pdk4 mRNAs were seen in the hypothalamus. These modest changes all appeared to be secondary to obesity rather than causative.

We then turned to genes in the pathway of the melanocortin-4/-3 receptor (Mc4r/3r) in the hypothalamus, known to play a pivotal role in maintaining energy homeostasis. Specifically, the mRNAs of the orexigenic neuropeptides AgRP and NPY genes were substantially increased in the hypothalamus of obese NEXLPL−/− mice at 6 months (Figure 4A), but another orexigenic neuropeptide melanin-concentrating hormone and the anorexigenic neuropeptide POMC were not affected. AgRP and NPY gene expression was also measured at 15 days and 3 months of age in the hypothalamus of NEXLPL−/− mice. At P15, there was no change in AgRP/NPY mRNA in NEXLPL−/− mice (data not shown), strongly suggesting that the modification of AgRP gene expression in adult mice was not developmental. However, interestingly, at 3 months and before the onset of obesity, AgRP levels were even more elevated in NEXLPL−/− mice (3.1-fold at 3 months versus 2.2-fold at 6 months) (Figure 4A). We also examined whether AgRP gene expression

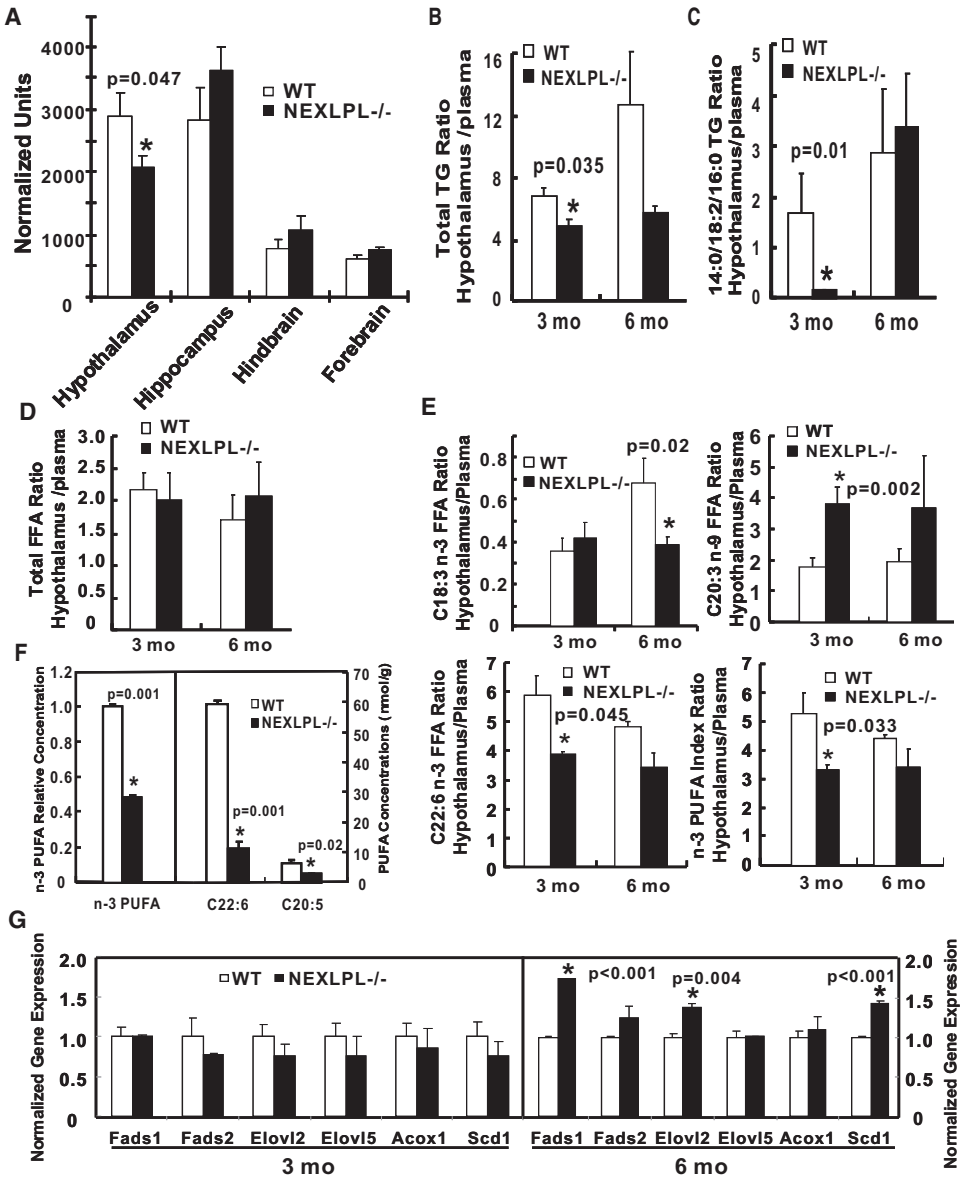

Figure 3. Brain Lipid Metabolism in NEXLPL–/– Mice at 3, 6, and 12 Months

(A) Reduction of TG-rich, lipoprotein-derived TG/FA uptake in the hypothalamus of NEXLPL−/− mice at 3 months (n = 7 for WT and n = 6 for NEXLPL−/−).

(B) Total TG concentrations in the hypothalamus of 3- and 6-month-old NEXLPL−/− mice.

(C) TG (18:2/14:0/16:0) in the hypothalamus of 3- and 6-month-old NEXLPL−/− mice.

(D) Total FFA concentrations in the hypothalamus of 3- and 6-month-old NEXLPL−/− mice.

(E) Deficiency of n-3 PUFAs in 3-month-old and 6-month-old NEXLPL−/− mice. n-3 index is percentage of all n-3 PUFAs in total FFA.

(F) n-3 PUFA deficiency in the hypothalamus of 12-month-old NEXLPL−/− mice (n = 2 for WT, n = 3 for NEXLPL−/−).

(G) PUFA biosynthetic enzyme pathway gene expression levels in the hypothalamus of 3- and 6-month-old NEXLPL−/− mice (n = 4). In all panels, n = 6 for WT; n = 4 for NEXLPL−/− for (B)–(E). Lipid levels in (A)–(E) are reported with hypothalamic lipid levels normalized to plasma levels. See also Figure S2 and Table S2. The error bars in this figure are SEM.

predicted obesity in NEXLPL+/− mice (Figure 4B). Indeed, AgRP gene expression was only somewhat higher in NEXLPL−/− mice at 3 months (1.5-fold), but was substantially increased at 6 months (7.7-fold, preobese and before the increases in food intake in these mice) and much less increased at 9 months (1.9-fold, after the increase in food intake was gone). AgRP is a natural antagonist of both Mc3r and Mc4r receptors. It was interesting to note that Mc3r but not Mc4r mRNA was increased nearly 2-fold by 6 months in NEXLPL−/− mice, and Mc3r was increased before the onset of obesity and remained elevated through the development of obesity (Figure 4C).

DISCUSSION

Previously, our lab demonstrated that LPL was expressed and synthesized in neurons in different brain regions (Eckel and

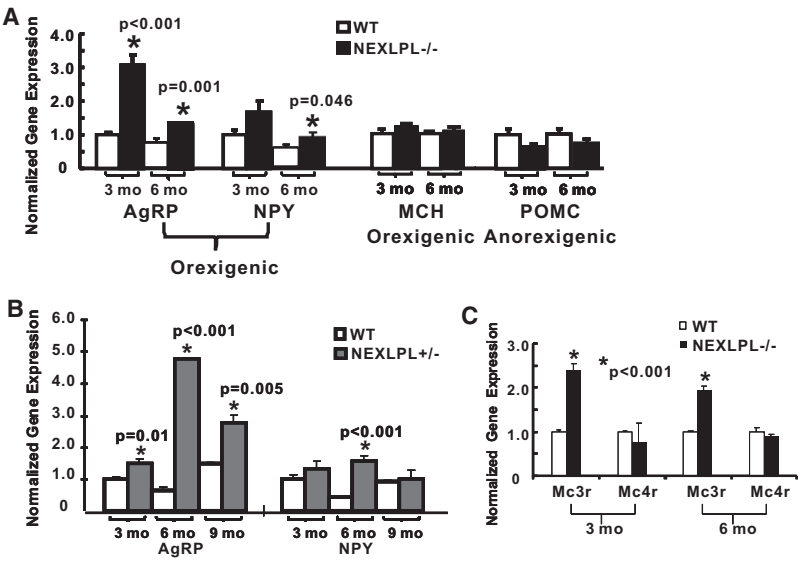

Figure 4. Gene Expression in NEXLPL–/– Mice Pre- and Post-Obesity Development

(A) Neuropeptide gene expression in the hypothalamus of NEXLPL−/− mice at 3 and 6 months.

(B) AgRP and NPY gene expression in the hypothalamus of NEXLPL+/− mice at 3, 6, and 9 months.

(C) Melenocortin-3 and -4 receptor gene expression in the hypothalamus of NEXLPL−/− mice at 3 and 6 months. n = 4 for each group of mice. See also Figure S3. The error bars in this figure are SEM.

Robbins, 1984; Bessesen et al., 1993; Goldberg et al., 1989). Moreover, we hypothesized that LPL in the brain could modulate appetite (Eckel and Robbins, 1984). LPL contributes in a major way to TG-rich lipoprotein metabolism, tissue-specific fuel delivery and utilization, and many aspects that relate to energy balance, insulin action, and body weight regulation; however, these roles have all been attributed to LPL in peripheral tissues. Some evidence, however, suggests a role of LPL in the brain. Mice heterozygous for generalized LPL deficiency have an age-dependent increase in the ratio of fat mass to lean mass (Chen et al., 2008), and although humans with homozygous LPL deficiency are typically not obese, patients with heterozygous LPL deficiency can be overweight or obese (Babirak et al., 1989; Julien et al., 1997). In these cases, LPL is absent or reduced in all tissues of the body, not just the neuron. We now have a neuronal-specific, LPL-deficient model to directly evaluate the in vivo function of LPL in the brain.

NEXLPL−/− mice developed obesity by 16 weeks on a chow diet, and the extent of obesity was the most severe among all existing LPL-deficient mouse models. This result indicates an important function of LPL in CNS neurons and the potential role of TG-rich lipoprotein metabolism as a mechanism of CNS regulation of energy balance and body weight. Furthermore, in most of the other genetically modified obesity mouse models, only male mice display the pronounced phenotype. In NEXLPL−/− mice, both males and females developed obesity at the same rate, with gender differences observed only in the plasma leptin and insulin levels at 6 months and the extra percentage of weight gain.

Both NEXLPL−/− and NEXLPL+/− mice developed obesity in a two-step time course with an increase in energy intake preceding the reduction in energy expenditure. Although the period of hyperphagia was not as well defined in younger NEXLPL−/− mice, we believe that this was mostly due to the faster rate of obesity development in combination with variances between mice. Because both energy intake and energy expenditure were modified in NEXLPL mice, it was important to note the substantial increases in AgRP and NPY gene expression before the onset of obesity and the persistent increase of these neuropeptides, albeit at a lower level, after obesity developed. A number of studies have indicated that upregulation of AgRP can increase energy intake as well as reduce energy expenditure (Small et al., 2001, 2003; Kaelin et al., 2004; Gropp et al., 2005; Semjonous et al., 2009). These reports provide a putative mechanism to explain why food intake and energy expenditure were both modified in NEXLPL mice.

The observation that the increase of AgRP gene expression was greater in preobese mice (NEXLPL−/− at 3 months and NEXLPL+/− at 6 months) than in obese mice (NEXLPL−/− at 6 months and NEXLPL+/− at 9 months) is of further interest. The initial higher levels of AgRP mRNA in the hypothalamus seemed to predict the subsequent increase in food intake to follow. Then, after the period of hyperphagia subsided and obesity developed, AgRP gene expression was reduced but still elevated. These results suggest that there are signals in neuronal LPL-deficient mice that can greatly upregulate the AgRP neurons early on, but these neurons are still responsive to some potential secondary signals that are likely to be compensatory in nature. It will be important for future studies to identify how neuron-specific reductions in LPL gene expression result in such pattern of regulation in AgRP neurons.

Besides the increases in AgRP gene expression, there was also a ~90% increase in expression of Mc3r but no change in the expression of Mc4r in both NEXLPL−/− and NEXLPL+/− mice, and this increase in Mc3r expression existed before the onset of obesity in NEXLPL−/− mice. Of note, AgRP acts as natural antagonist at the level of both Mc3 and Mc4 receptors. The increased expression of Mc3r could very well be a compensatory effect of the substantially increased gene expression of AgRP in the hypothalamus, which seems to have no effect on Mc4r expression. Compared to the important role of the Mc4r in regulating food intake and the CNS regulation of glucose homeostasis, the biological function of the Mc3r is not well established (Bolze and Klingenspor, 2009; Lee and Wardlaw, 2007). Mc3r is often colocalized with Mc4r and in some cases might share redundant functions with Mc4r, but accumulating data show that its precise function in obesity, cachexia, and related feeding behaviors might involve unique signaling pathways and/or regulatory mechanisms. Our mouse might prove to be the model to uncover the complex role of Mc3r in the regulation of energy balance and body weight. Furthermore, the selective activation of AgRP versus POMC neuronal activity in

the setting of no change in plasma glucose provides more evidence to support that AgRP neurons (and Mc3r) are more sensitive to lipid-derived signals in the brain than POMC neurons (and Mc4r) that preferentially sense glucose.

Considering the key role of LPL in peripheral tissues in regulating TG-rich lipoprotein-derived lipids for storage and/or oxidation, it is plausible that LPL contributes to the regulation of TG-rich lipoprotein metabolism in the brain. This is exactly what we have found in NEXLPL−/− mice. Despite the potential requirement of active transport of lipid molecules across the blood-brain barrier, our data suggest that brain tissue is not only capable of taking up lipids derived from TG-rich lipoproteins, but also this process is LPL dependent. Importantly, only PUFA metabolism seemed to be affected by neuronal LPL deficiency. This raises the intriguing possibility that LPL might play a more specific role in the regulation of the turnover of particular lipid species in the murine brain.

PUFAs are usually obtained from the diet or synthesized in the liver by elongation and desaturation of diet-derived 18:2 or 18:3 FFAs. Various elongase and desaturase enzymes have been found in the brain, where their activities do not appear to be modified by diet-induced obesity (Igarashi et al., 2007). In NEXLPL−/− mice, however, in addition to the earlier deficiency of a TG and n-3 PUFA, we also observed an increase in both desaturase and elongase gene expression in the hypothalamus but not in liver. A plausible interpretation is that an initial LPL-dependent defect in the hypothalamic uptake of the essential dietary TG and FAs in NEXLPL mice is followed by a compensatory upregulation of enzymes in the PUFA biosynthetic pathway. As the NEXLPL−/−mice age and become more obese, the dramatic drop in n-3 PUFA content in the hypothalamus indicates either a slower production of n-3 PUFAs and/or a faster rate of n-3 PUFA turnover.

Recently, long-chain PUFA have been shown to play a key role in the control of body fat by regulating the expression of lipid- and lipoprotein-related genes (Jump, 2008; Sampath and Ntambi, 2004) as well as key neuropeptides that are involved in regulating energy balance and body weight (Wang et al., 2002; Dziedzic et al., 2007). Our results indicate that LPL might be regulating the availability of free long-chain PUFAs in the brain. Thus, the observed decrease in long-chain PUFAs in the hypothalamus of NEXLPL mice strongly suggests that the brain of these animals is unable to sense circulating lipoprotein-associated FAs and consequently increases the expression of orexigenic neuropeptides such as AgRP/NPY. Of interest, the AgRP gene has a 21 nucleotide sequence that is 100% identical to the sequence found in the promoter of the neuron-derived orphan receptor-1 (NOR-1) (Brown et al., 2001), and NOR-1 action is preferentially inhibited by n-6 and n-3 FAs (Maxwell and Muscat, 2006). Notably, the fact that the lipid metabolism in the liver of NEXLPL mice remains unchanged indicates that the reduction in long-chain PUFAs in the hypothalamus is secondary to an LPL-related defect in the CNS.

In summary, neuron-specific reductions in LPL gene expression in mice result in severe obesity. This phenotype appears to be biphasic, with a period of increased food intake followed by more sustained reductions in physical activity and MR. This progressive change in energy balance may be due to the LPL-dependent decrease in PUFA levels and increased AgRP/NPY gene expression in the hypothalamus. Overall, our study opens the door to a previously undiscovered CNS pathway that regulates energy balance and body weight.

EXPERIMENTAL PROCEDURES

Generation of NEXLPL–/– and NEXLPL+/– Mice

In brief, the CNS neuronal-specific LPL-depleted mice (NEXLPL−/−) were generated by crossing the LPL *loxP* mice (Augustus et al., 2004) with transgenic mice having the brain-specific expression of cre recombinase driven by the regulatory sequences of NEX, a gene that encodes a neuronal basic helix-loop-helix (bHLH) protein (Goebbels et al., 2006).

LPL Activity Assay

After a 4 hr fast, mice were anesthetized with an i.p. administration of Avertin (2,2,2-tribromoethanol, 250 mg/kg). Tissues were dissected and assayed immediately. Heparin-releasable LPL activity was measured in brain regions and in peripheral tissues as previously described (Jensen et al., 2008). LPL activity was expressed as nmoles of FFA per minute per gram tissue.

Measurement of Body Weight, Body Composition, and Plasma Metabolic Parameters

Body weight was monitored on a weekly basis for individualized caged mice. Body composition was measured on anesthetized mice by dual-energy X-ray absorptiometry using a mouse densitometer (PIXImus2, Lunar Corp.; Madison, WI). Plasma samples were collected after a 4 hr fast, and metabolic parameters were measured as previously described (Wang et al., 2009).

Indirect Calorimetry and Physical Activity Measurements

An open-ended indirect calorimetry system coupled with Columbus Instruments Opto M3 multichannel activity monitor was used to measure average daily food intake, oxygen consumption (O_2) and carbon dioxide (CO_2) production in mice to calculate MR and RQ, and physical activity as described in Supplemental Experimental Procedures.

Quantitative Real-Time PCR

Different regions of the brain were collected from 6-month-old anesthetized mice after a 4 hr fast, flash frozen, and stored at −80°C until processing. Total RNA was extracted from homogenized tissue using both TRIzol reagent (Invitrogen) and RNeasy Mini Kit (QIAGEN). Reverse transcription was performed using 1 μg total RNA with iScript cDNA synthesis kit (Bio-Rad). Quantitative PCR was performed using primer sets for genes of interest and three reference genes and iQ Supermix or iQ SYBR Supermix (Bio-Rad) following the manufacturer's protocols.

Lipidomic Analyses of Brain Tissues

Mice were fasted for 4 hr, anesthetized, and decapitated, and brains were quick-frozen in 2-methylbutane at −40°C and then stored at −80°C until further processing. Brain regions were punched from the frozen brains using cryo-cut and cylindrical brain punchers (Fine Science Tools; Foster City, CA). Frozen punches were weighed and homogenized in methanol containing the following internal standards: d_8-arachidonic acid, d_8-2-arachidonoyl glycerol (Cayman Chemical; Ann Arbor, MI), diheptadecanoin, trinonadecenoin (Nu-Chek Prep; Elysian, MN). Lipids were analyzed as previously described (Astarita et al., 2009). Briefly, lipids were extracted with chloroform (2 vol) and washed with water (1 vol). Organic phases were collected and dried under liquid nitrogen. Lipids were reconstituted in chloroform/methanol (1:4, vol/vol) for liquid chromatography/mass spectrometry (LC/MS) analyses. Lipid identification and quantification are described in the Supplemental Experimental Procedures.

Preparation of Radiolabeled CMs and In Vivo Uptake

Endogenously radiolabeled CMs were prepared as described in the Supplemental Experimental Procedures and then injected into 4 hr fasted mice via the tail vein at time 0, with each mouse receiving 2 × 10^6 dpm of [^{3}H]triolein-labeled CMs. Blood was collected at 0.5, 5, and 15 min after injection. At 15 min, hearts were perfused with cold PBS and tissues were harvested, flash

frozen in liquid nitrogen, and stored at −80°C until use. Radioactivity was determined in 10 μl plasma and 100 μl tissue homogenate on a LS 6500 multipurpose scintillation counter (Beckman Coulter; Brea, CA). Tissue uptake of the radiolabeled triolein in CMs was normalized per gram of tissue and then normalized to plasma radioactivity at 30 s (dpm/ml) for each mouse.

Statistical Analyses

Results are presented as mean ± SEM. The error bars in all figures are SEM. t tests were performed using SigmaStat 2.03 (San Rafel, CA). A $p < 0.05$ was considered significant.

SUPPLEMENTAL INFORMATION

Supplemental Information includes Supplemental Experimental Procedures, Supplemental References, three figures, and one table and can be found with this article online at doi:10.1016/j.cmet.2010.12.006.

ACKNOWLEDGMENTS

We wish to thank Jennifer H. Yoon, Dalan R. Jensen, and Daniel Bessesen for help with the breeding and genotyping of mice, maintenance of the calorimeter, and brain dissections. We thank Rachel C. Janssen at the Metabolic Core Laboratory at the University of Colorado Anschutz Medical Campus Nutrition Obesity Research Center (NIH-P30DK048520) for performing all the RT-PCR reactions and related data analyses. We thank the Agilent Technologies/University of California Irvine Analytical Discovery Facility, the Center for Drug Discovery, and the Agilent Technologies Foundation for the lipomics analysis. We also thank the Academic Enrichment Fund from the Dean's Office at the University of Colorado, School of Medicine for Bridge Funding and Kristin Eckel-Mahan at the University of California Irvine for her suggestion that we obtain the NEX cre recombinase mouse to create the neuron-specific LPL knockout mouse. This work was supported by DK42266 (R.H.E.), HL45095 (I.J.G.), and DK073955 (D.P.). K.G.B. was supported by a mentored postdoctoral fellowship from the American Diabetes Association.

Received: November 19, 2009
Revised: August 24, 2010
Accepted: November 4, 2010
Published: January 4, 2011

REFERENCES

Astarita, G., Ahmed, F., and Piomelli, D. (2009). Lipidomic analysis of biological samples by liquid chromatography coupled to mass spectrometry. Methods Mol. Biol. *579*, 201–219.

Augustus, A., Yagyu, H., Haemmerle, G., Bensadoun, A., Vikramadithyan, R.K., Park, S.Y., Kim, J.K., Zechner, R., and Goldberg, I.J. (2004). Cardiac-specific knock-out of lipoprotein lipase alters plasma lipoprotein triglyceride metabolism and cardiac gene expression. J. Biol. Chem. *279*, 25050–25057.

Babirak, S.P., Iverius, P.H., Fujimoto, W.Y., and Brunzell, J.D. (1989). Detection and characterization of the heterozygote state for lipoprotein lipase deficiency. Arteriosclerosis *9*, 326–334.

Ben Zeev, O., Doolittle, M.H., Singh, N., Chang, C.H., and Schotz, M.C. (1990). Synthesis and regulation of lipoprotein lipase in the hippocampus. J. Lipid Res. *31*, 1307–1313.

Bessesen, D.H., Richards, C.L., Etienne, J., Goers, J.W., and Eckel, R.H. (1993). Spinal cord of the rat contains more lipoprotein lipase than other brain regions. J. Lipid Res. *34*, 229–238.

Bolze, F., and Klingenspor, M. (2009). Mouse models for the central melanocortin system. Genes Nutr. *4*, 129–134.

Brown, A.M., Mayfield, D.K., Volaufova, J., and Argyropoulos, G. (2001). The gene structure and minimal promoter of the human agouti related protein. Gene *277*, 231–238.

Caspi, L., Wang, P.Y., and Lam, T.K. (2007). A balance of lipid-sensing mechanisms in the brain and liver. Cell Metab. *6*, 99–104.

Chen, Y., Zhu, J., Lum, P.Y., Yang, X., Pinto, S., MacNeil, D.J., Zhang, C., Lamb, J., Edwards, S., Sieberts, S.K., et al. (2008). Variations in DNA elucidate molecular networks that cause disease. Nature *452*, 429–435.

Dziedzic, B., Szemraj, J., Bartkowiak, J., and Walczewska, A. (2007). Various dietary fats differentially change the gene expression of neuropeptides involved in body weight regulation in rats. J. Neuroendocrinol. *19*, 364–373.

Eckel, R.H., and Robbins, R.J. (1984). Lipoprotein lipase is produced, regulated, and functional in rat brain. Proc. Natl. Acad. Sci. USA *81*, 7604–7607.

Goebbels, S., Bormuth, I., Bode, U., Hermanson, O., Schwab, M.H., and Nave, K.A. (2006). Genetic targeting of principal neurons in neocortex and hippocampus of NEX-Cre mice. Genesis *44*, 611–621.

Goldberg, I.J., Soprano, D.R., Wyatt, M.L., Vanni, T.M., Kirchgessner, T.G., and Schotz, M.C. (1989). Localization of lipoprotein lipase mRNA in selected rat tissues. J. Lipid Res. *30*, 1569–1577.

Gropp, E., Shanabrough, M., Borok, E., Xu, A.W., Janoschek, R., Buch, T., Plum, L., Balthasar, N., Hampel, B., Waisman, A., et al. (2005). Agouti-related peptide-expressing neurons are mandatory for feeding. Nat. Neurosci. *8*, 1289–1291.

Igarashi, M., Ma, K., Chang, L., Bell, J.M., and Rapoport, S.I. (2007). Dietary n-3 PUFA deprivation for 15 weeks upregulates elongase and desaturase expression in rat liver but not brain. J. Lipid Res. *48*, 2463–2470.

Jensen, D.R., Knaub, L.A., Konhilas, J.P., Leinwand, L.A., MacLean, P.S., and Eckel, R.H. (2008). Increased thermoregulation in cold-exposed transgenic mice overexpressing lipoprotein lipase in skeletal muscle: an avian phenotype? J. Lipid Res. *49*, 870–879.

Julien, P., Vohl, M.C., Gaudet, D., Gagne, C., Levesque, G., Despres, J.P., Cadelis, F., Brun, L.D., Nadeau, A., and Ven Murthy, M.R. (1997). Hyperinsulinemia and abdominal obesity affect the expression of hypertriglyceridemia in heterozygous familial lipoprotein lipase deficiency. Diabetes *46*, 2063–2068.

Jump, D.B. (2008). N-3 polyunsaturated fatty acid regulation of hepatic gene transcription. Curr. Opin. Lipidol. *19*, 242–247.

Kaelin, C.B., Xu, A.W., Lu, X.Y., and Barsh, G.S. (2004). Transcriptional regulation of agouti-related protein (Agrp) in transgenic mice. Endocrinology *145*, 5798–5806.

Lee, M., and Wardlaw, S.L. (2007). The central melanocortin system and the regulation of energy balance. Front. Biosci. *12*, 3994–4010.

Loftus, T.M., Jaworsky, D.E., Frehywot, G.L., Townsend, C.A., Ronnett, G.V., Lane, M.D., and Kuhajda, F.P. (2000). Reduced food intake and body weight in mice treated with fatty acid synthase inhibitors. Science *288*, 2379–2381.

Maxwell, M.A., and Muscat, G.E. (2006). The NR4A subgroup: immediate early response genes with pleiotropic physiological roles. Nucl. Recept. Signal. *4*, e002.

Morgan, K., Obici, S., and Rossetti, L. (2004). Hypothalamic responses to long-chain fatty acids are nutritionally regulated. J. Biol. Chem. *279*, 31139–31148.

Obici, S., Feng, Z., Morgan, K., Stein, D., Karkanias, G., and Rossetti, L. (2002). Central administration of oleic acid inhibits glucose production and food intake. Diabetes *51*, 271–275.

Obici, S., Feng, Z., Arduini, A., Conti, R., and Rossetti, L. (2003). Inhibition of hypothalamic carnitine palmitoyltransferase-1 decreases food intake and glucose production. Nat. Med. *9*, 756–761.

Parton, L.E., Ye, C.P., Coppari, R., Enriori, P.J., Choi, B., Zhang, C.Y., Xu, C., Vianna, C.R., Balthasar, N., Lee, C.E., et al. (2007). Glucose sensing by POMC neurons regulates glucose homeostasis and is impaired in obesity. Nature *449*, 228–232.

Sampath, H., and Ntambi, J.M. (2004). Polyunsaturated fatty acid regulation of gene expression. Nutr. Rev. *62*, 333–339.

Sandoval, D., Cota, D., and Seeley, R.J. (2008). The integrative role of CNS fuel-sensing mechanisms in energy balance and glucose regulation. Annu. Rev. Physiol. *70*, 513–535.

Schwartz, M.W., and Porte, D., Jr. (2005). Diabetes, obesity, and the brain. Science *307*, 375–379.

Semjonous, N.M., Smith, K.L., Parkinson, J.R., Gunner, D.J., Liu, Y.L., Murphy, K.G., Ghatei, M.A., Bloom, S.R., and Small, C.J. (2009). Coordinated changes in energy intake and expenditure following hypothalamic administration of neuropeptides involved in energy balance. Int. J. Obes. (Lond) *33*, 775–785.

Small, C.J., Kim, M.S., Stanley, S.A., Mitchell, J.R., Murphy, K., Morgan, D.G., Ghatei, M.A., and Bloom, S.R. (2001). Effects of chronic central nervous system administration of agouti-related protein in pair-fed animals. Diabetes *50*, 248–254.

Small, C.J., Liu, Y.L., Stanley, S.A., Connoley, I.P., Kennedy, A., Stock, M.J., and Bloom, S.R. (2003). Chronic CNS administration of Agouti-related protein (Agrp) reduces energy expenditure. Int. J. Obes. Relat. Metab. Disord. *27*, 530–533.

Smit, E.N., Muskiet, F.A., and Boersma, E.R. (2004). The possible role of essential fatty acids in the pathophysiology of malnutrition: a review. Prostaglandins Leukot. Essent. Fatty Acids *71*, 241–250.

Wang, H., and Eckel, R.H. (2009). Lipoprotein lipase: from gene to obesity. Am. J. Physiol. Endocrinol. Metab. *297*, E271–E288.

Wang, H., Storlien, L.H., and Huang, X.F. (2002). Effects of dietary fat types on body fatness, leptin, and ARC leptin receptor, NPY, and AgRP mRNA expression. Am. J. Physiol. Endocrinol. Metab. *282*, E1352–E1359.

Wang, H., Knaub, L.A., Jensen, D.R., Young, J.D., Hong, E.G., Ko, H.J., Coates, A.M., Goldberg, I.J., de la Houssaye, B.A., Janssen, R.C., et al. (2009). Skeletal muscle-specific deletion of lipoprotein lipase enhances insulin signaling in skeletal muscle but causes insulin resistance in liver and other tissues. Diabetes *58*, 116–124.